COMPREHENSIVE WELDABILITY ANALYSIS AND MORPHOLOGICAL-THERMAL INSIGHTS INTO ULTRASONIC WELDING OF ABS FOR ELECTRONICS APPLICATIONS

UDC:621.791.1:621.38
Original scientific paper https://doi.org/10.46793/aeletters.2025.10.3.1

Sharanabasavaraj Radder[1*], Mukti Chaturvedi[1], S. Arungalai Vendan[1]

[1] Electronics and Communication Department, Dayananda Sagar University, Bangalore, Karnataka, India

Abstract:
The use of ultrasonic welding for joining thermoplastic materials has also attracted much interest as a precise and efficient method. This study examines the application of ultrasonic welding in the production of casings for power circuits in battery chargers, utilising Acrylonitrile Butadiene Styrene (ABS) material. Systematic control experiments have been carried out with energy, weld time, and hold time variations to investigate their influence on weld properties. The weld test pieces were evaluated using both destructive and non-destructive testing methods to determine their quality and assess the effects of pressure and thermal gradients on the microstructure of the weld. The analysis techniques employed are X-ray diffraction (XRD), Fourier Transform Infrared Spectroscopy (FTIR), Scanning Electron Microscopy (SEM), Thermogravimetric Analysis (TGA), and Atomic Force Microscopy (AFM). Based on a detailed analysis of the experimental results, the present study offers valuable information concerning the effect of process parameters on the morphology of ABS material battery charger casings. This study showed microstructural and thermal modifications in ABS. Non-optimal parameters may result in localized chain reorientation and nanoscale porosity at the weld interface. The welding procedure preserved the polymer chemistry, but rapid heating and cooling caused localized property alterations, owing to welding-induced phase separation. The conclusions drawn from this research can guide future investigations and advance industrial practices aimed at optimizing the ultrasonic welding process for ABS materials in the context of specific device production.

ARTICLE HISTORY
Received: 10 May 2025
Revised: 8 July 2025
Accepted: 23 July 2025
Published: 30 September 2025

KEYWORDS
Ultrasonic Welding, Electronics components, Molecular Bonds, control mechanisms, Battery charger, Piezoelectric crystal, TGA, SEM, AFM, XRD

1. INTRODUCTION

Ultrasonic welding is a crucial process step in the latest production methodology, offering a significant balance of cost, accuracy, speed, and reliability for joining polymeric materials. The ultrasonic welding technique utilizes the frictional heat created by high-frequency vibrations to form a molecular bond in polymers [1,2]. The vibrations are generated in the transducer, which is a stack of piezoelectric discs subjected to a supply voltage. The vibration amplitude can be used to estimate the heat generated in the ultrasonic welding process. This will help in establishing the correlation between the heat generated and the weld strength. The obtained correlation can be used to identify the optimal parametric range for generating the maximum heat and hence yielding the maximum strength of the weld.

The ultrasonic-frequency vibrations produce a localized rise in temperature and molecular diffusion of particles, which results in the bonding of the polymer components. Ultrasonic welding is a preferred joining technique for manufacturing

*CONTACT: Sharanabasavaraj Radder, e-mail: sharanabasava-ece@dsu.edu.in

battery charger casings because it produces solid and reliable welds with minimal thermal distortion and high production rates [3,4]. The power source provides electrical signals between 15 kHz and 70 kHz, depending on the crystal specifications [5,6]. The frequency of operation plays a critical role in determining the performance and efficiency of ultrasonic welding [1,2]. ABS is widely utilized for both exterior and interior components in the automotive industry because of its resistance to mechanical loading and harsh climatic conditions. Owing of its superior moldability, visual attractiveness, and surface smoothness, ABS is frequently used in consumer electronics to fabricate casings, enclosures, and structural components [7-10]. It must be highly resistant to heat to function at the high temperatures produced during operation without deforming or deteriorating. The battery converter must provide sufficient electrical insulation to protect against risks and ensure a safe working environment.

Testing and characterization techniques are essential to test the properties of weld samples, optimize the process and its parameters, and ensure the reliability and quality of produced products in various applications. Weld microstructure, shape, interface bonding, and defects such as voids, pores, or incomplete fusion can be analyzed through microscopic testing. Fourier Transform Infrared Spectroscopy (FTIR) analyzes the chemical structure in the surrounding regions and the weld interface. It gives insights into dynamics within the welding process and performance of the material by helping to determine molecular changes, chemical bonding, and potential degradation or contamination. Differential Scanning Calorimetry (DSC) was conducted to determine the thermal characteristics of the weld, including its melting point, crystallinity, and thermal stability. Thermogravimetric Analysis (TGA) was used to test the thermal stability and degradation behaviour of the weld. It assists in determining the decomposition temperature, degradation rate, and residual mass, and can indicate the weld's thermal performance and long-term stability [11]. Atomic Force Microscopy (AFM) has been used to investigate the roughness, texture, and defects of the polymer weld. It shows the degree of polymer fusion and any gaps, voids, or phase separations at the interface [12].

Researchers have enabled advancements in ultrasonic welding with various technological innovations. The development of advanced control mechanisms for controlling parameters such as vibration frequency, amplitude, welding force, and duration has enabled operators to tailor the welding process to suit specific materials and geometries [13-15].

Sophisticated monitoring and recording methods have been incorporated into ultrasonic welding machines to record the values of parameters and monitor the performance of the weld process [12-14,16]. In addition, enhancements in booster design and materials for the sonotrode have improved the performance and consistency of ultrasonic welding machines [11,17,18]. The study by Rajkumar et al. [19] optimized the ultrasonic welding (USW) parameters such as welding time, amplitude, axial pressure, and holding time to increase automotive ABS plastic lap joint tensile shear fracture load (TSFL). Yang and Yang [20] suggested that the energy absorption of ultrasonic waves primarily targets material defects, transferring energy to the crystalline lattices or amorphous main chains. Villegas [21] reviewed the main aspects of the USW process, including energy directors and process parameters, and inferred that Simplified solutions, such as flat energy directors, can accommodate stiffness variations. Yang et al. [22] examined the contact behaviour and temperature characteristics utilizing the harmonic balancing approach and observed that the contact force rises during the horn plunging process. Amplitude and welding time notably impact surface temperature, with the effect of plunging speed being minimal and the effect of trigger force being negligible. Rogale et al. [23], in their study, identified 44 key process variables for polymer welding, divided into three groups: material-specific parameters (12), acoustic/electroacoustic parameters (11), and machine-specific parameters (21). Kuo et al. [24] found that amplitude was the most critical control element determining ultrasonic weld strength, followed by weld pressure, hold time, and trigger position. Vendan et al. [25] conducted experimental work to study the blends of PC and ABS sheets in a 60:40 ratio, which are ultrasonically welded and used ANN and ANFIS techniques to analyse tensile strength, with ANFIS outperforming ANN.

In the current industrial practices, the trial-and-error method is commonly employed to determine the optimal parameters for any process. This can lead to random attempts, time wastage, and energy expenditure for the repetition of the weld sequence. Further research is needed to optimize the process parameters for specific materials, geometries, and applications. This work is an

attempt to address a few of the research gaps using experimental trials with variation of process parameters for obtaining optimal parametric range, and assessment of welds to establish the protocols and procedures for assessment. It also includes the determination of power usage and analysis of aspects leading to unwanted welds. The following section provides information about the experimental work, results, testing and characterization details, and the inferences drawn from the experimental work.

2. MATERIALS AND METHODS

The main components of a typical ultrasonic welding machine, as shown in Fig. 1, include piezoelectric crystals as a converter, boosters, a sonotrode (or horn), and an anvil [2]. A converter is used to convert an electrical power signal into high-frequency vibrations. The booster reinforces these vibrations and passes them to the Sonotrode, which causes bond formation in the workpiece with the effect of heat and pressure [26]. Empirical values of the frictional and viscoelastic heat generated per unit area per unit time is given by Eqs. 1 and 2 [3]:

$$\dot{q_f} = \frac{(\alpha^2 \cdot \mu \cdot \omega \cdot A \cdot \sigma_o)}{\pi}, \quad (1)$$

where are:
α - hammering displacement coefficient (dimensionless),
μ - friction coefficient (dimensionless),
A - average slippage amplitude (μm),
ω - vibration frequency (kHz),
σ_o - interfacial pressure (Pa);

$$q_v = \frac{1}{2} \cdot (\alpha^2 \cdot \omega \cdot \mathrm{E}'' \cdot B^2), \quad (2)$$

where are:
E'' - loss modulus (Pa),
B - strain amplitude (dimensionless).

As per the piezoelectric characteristics, the displacement induced in the piezoelectric crystals is in direct proportion to the applied motional voltage, Eq. [3]:

$$Amplitude\ \delta = d \cdot Va, \quad (3)$$

where are:
d - piezoelectric constant (μm/V)
V_a - applied voltage (V).

The configuration and parameter ranges of the machine components are guided by the material qualities, weld shape and geometry. Furthermore, the selection of specifications for power converters [3,4] and piezoelectric crystals directly affects the effectiveness of ultrasonic welding processes that need to be carefully considered during device design and configuration.

Experiments were conducted at Dayananda Sagar University, Bangalore. The machine used for joining the polymer was 25 kHz, 120 kVA ultrasonic machine provided by Ultratechsonic Solutions, Bangalore. Its components and other key specifications are presented in Fig. 2 and Table 1.

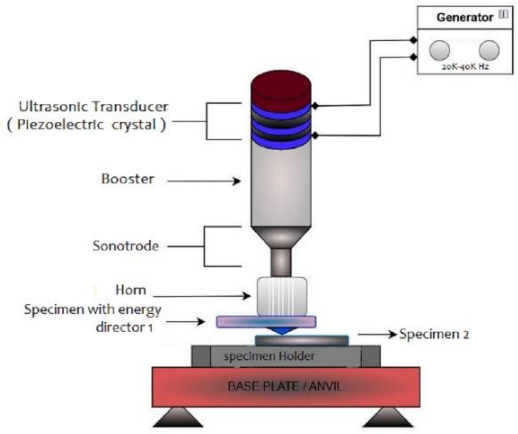

Fig. 1. Schematic of USW machine and technique

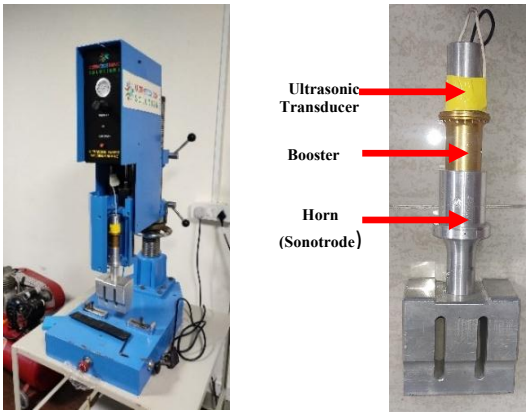

Fig. 2. Ultrasonic Welding Machine used for experimental trials

Table 1. Ultrasonic Machine Details

Operating frequency (kHz)	Maxim force (N)	Weight of machine (kg)	Weld generator-max. power output (W)	Weight of horn (kg)
20	3000	115	900/2000/3000	6

Welding was done for ABS material having the form and shape as shown in Fig. 3a. The dimensions of the battery charger casing, in Fig. 3b, are 5”x3”x1”. Experimental trials were made with the variation of the following control parameters, Table 2.

Table 2. Variation of Values of Process Parameter for the welding of Charger casing

No	Test identification	Delay time (s)	Weld time (s)	Holding time (s)	Current (mA)	Clamp pressure (bar)	Power (W)	Weld Status based on DT*	Observation on repeatability (Trials made with the same input parametric values)
1	1A	0.5	2	1.5	0.2	2	2	N.W	Achieved Repeatability
2	1B					3	2	N.W	
3	1C					4	2	N.W	
4	2A	0.5	2	1.5	0.2	2	3	N.W	
5	2B					3	3	N.W	
6	2C					4	3	N.W	
7	3A	0.5	2	1.5	0.2	2	4	N.W	
8	3B					3	4	N.W	
9	3C					4	4	P.W	
10	4A	0.5	2	1.5	0.5	2	2	P.W	
11	4B					3	2	P.W	Small Variations
12	4C					4	2	P.W	
13	5A	0.5	2	1.5	0.5	2	3	P.W	
14	5B					3	3	G.W	
15	5C					4	3	G.W.H	Small Variations
16	6A	0.5	2	1.5	0.5	2	4	G.W.H	
17	6B					3	4	G.W.V.H	Achieved Repeatability
18	6C					4	4	G.W.V.H	

The pressure, time parameters of weld, delay, and hold, as well as amperage and power input, resulted in varied weld strengths for each case. With reference to earlier experimental studies on the ultrasonic welding of the same material in a similar configuration, the operating ranges of these parameters were estimated by trial and error for the battery charger casing sample.

The weld status in Table 2 has the following observations: N.W - No weld, P.W - Partial weld, G.W.H - Good weld with high strength, G.W.V.H- Good weld with very high strength.

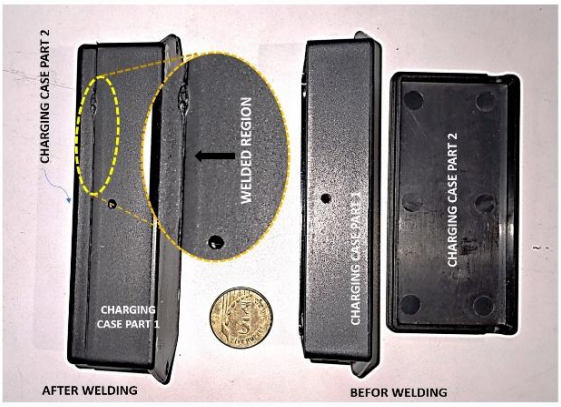

a)

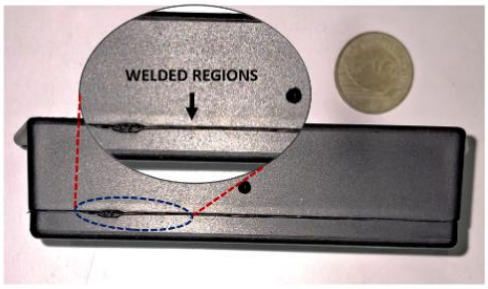

b)

Fig. 3. a) Battery Charger Casing, b) Weld specimens tested and characterized

3. RESULTS AND DISCUSSIONS

Based on visual inspection, samples with Good Weld and high strength were tested and characterised. Testing and characterisation were used to understand weld characteristics and find welding process improvements.

3.1 SEM Analysis

Scanning Electron Microscopy (SEM) imaging of various samples (Figs. 4-8) has enabled detailed analysis of the effects of heat generated with friction and viscous effects on the surface of the ABS material at different positions along the joint. An SEM image of an unwelded ABS sample was considered as the reference image, for comparison with the material microstructure

post-welding, Fig. 4. The SEM image reveals a smooth surface characterized by particle-like features, possibly due to the sample preparation dynamics and the surface finish of the molding die. In Fig. 5, the white particles indicate the peaks, with higher peaks signifying favorable melting conditions of the energy directors.

A prominent characteristic of the welded samples is the distorted ridges in Fig.6. The quantity and depth of these deformed ridges are directly related to the welding time, temperature, and weld pressure. The observations indicate that no impurities or complex substances are present that could compromise the welds. A fusion zone with varying textures appeared on the surface, owing to the melting and solidification dynamics in the material. The rapid cooling and localized heating that occur during the ultrasonic welding process can be attributed to be the cause of these characteristics. Flow marks were visible on the weld line, indicating that the polymer melted and flowed before solidifying. Porous surface and micro-voids are observed along the weld line.

Fig. 4. SEM image of the original ABS base sample

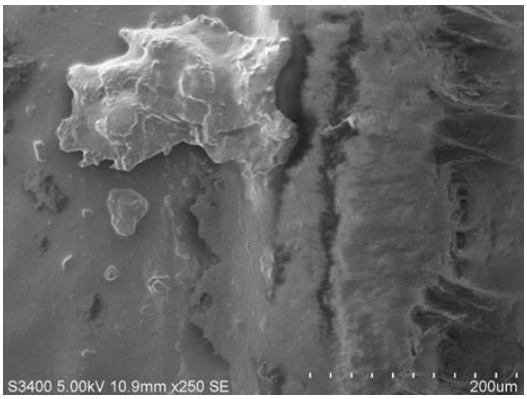

Fig. 5 SEM image of sample 2c at anomaly position 1

Fig. 6. SEM image of sample 2c at anomaly position 2

The microstructure showed the dispersed phases, particularly the rubbery particles inside the ABS. At lower magnifications, there were no visible gaps at the interface between the welded sections, indicating a successful weld with close surface contact. Surface roughness variations were observed throughout the weld, owing to the uneven heating and cooling rates during the welding procedure. Microcracks in Fig.7, were visible in some areas, which may have been due to the high-frequency vibrations during the welding process. Next to the fusion zone, a clear heat-affected zone (HAZ) is observed in Fig. 8. The HAZ polymer appeared partially melted due to ultrasonic welding heat, showing thermal deterioration. The welded sample had brittle morphology, with fracture-prone spots in the ABS polymer phase with increased styrene. The increased melt flow thrust outward during welding causes weld flash on the sample's surface. Variation in the bond line thickness indicates energy absorption and dispersion across the weld. Beyond the HAZ, the overall micro-structure remained intact close to the weld, indicating little thermal degradation. Strong adhesion was seen in some areas, which suggests effective energy transfer and fusion. The wave-like patterns observed on the surface are consistent with the high-frequency oscillations in Ultrasonic welding.

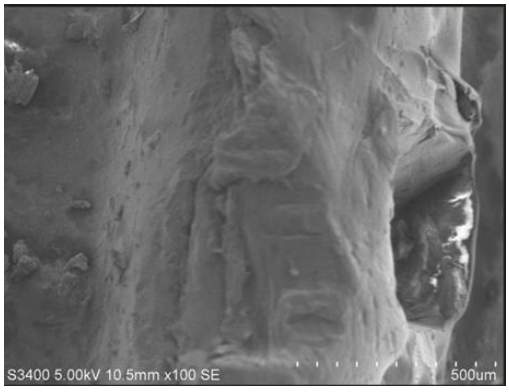

Fig. 7. SEM image of sample 3c at anomaly position 1

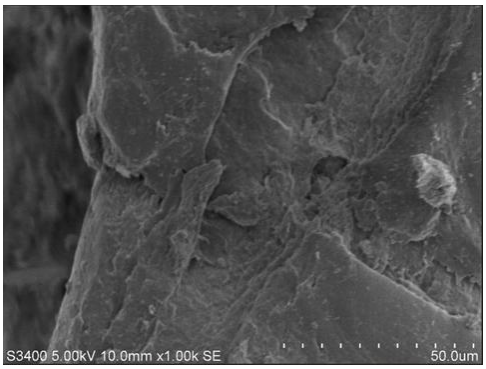

Fig. 8. SEM image of sample 3c at anomaly position 2

3.2 FTIR Analysis

FTIR analysis is employed to compare samples with the reference image of the material. FTIR analysis of the weld gives useful information on chemical composition, additives, degradation products, molecular structures, and interface binding. The FTIR spectrum gives information regarding weld heating-induced changes, assists in identifying the influence of welding parameters on weld characteristics, detects possible irregularities or changes, optimizes the welding parametric window, and thus enables consequent high-quality weld seams of ABS polymer parts [27]. The peaks in the FTIR spectrum are associated with distinct vibrational modes of the functional groups. They give significant details regarding material composition and its molecular arrangements. The broadened peak reflects the modulations that occur in the material during ultrasonic welding. The intensity variation in the FTIR plot indicates the possibility of decomposition of components that can happen as a result of high-energy inputs by ultrasonic welding. The default peaks of the ABS, C-H and C-C components, as well as other key parameters, were measured for the unwelded ABS samples.

The main peak in the FTIR spectra of ABS sample 2c is found at a wave number of 800 cm^{-1}, representing absorption due to the bending vibration of aromatic C-H bonds. This indicates the occurrence of aromatic CH out-of-plane bending, as ABS is a mixture of cis, trans, and vinyl isomers with both linear and cross-linked structures [28].

FTIR spectroscopy indicates the chemical and physical changes induced by the ultrasonic welding. Broadened peaks, variation in intensity, and minor shifts are some of the observations that reveal cross-linking and considerable thermal degradation (Figs. 9-11).

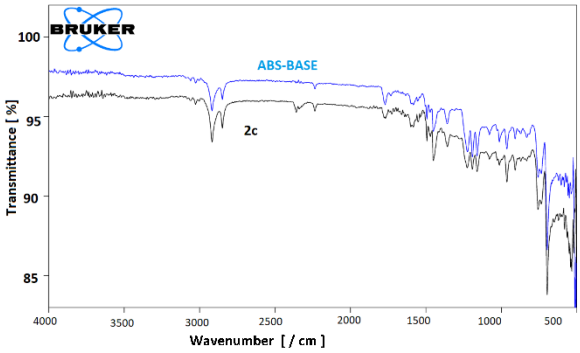

Fig. 9. FTIR plot for Sample 2c

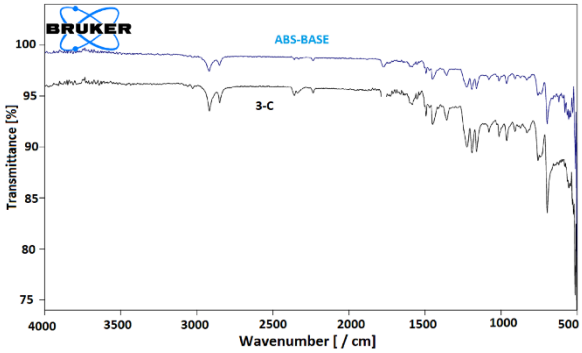

Fig.10. FTIR plot for Sample 3c

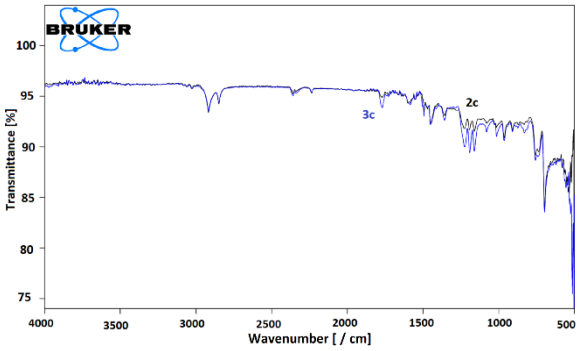

Fig. 11. FTIR Comparison chart for both samples

3.3 X-RAY DIFFRACTION

XRD scans were obtained for the base material as well as for the samples selected for the weld with varying parametric set values, Fig. 12-14. The peaks obtained provide insight into the polymer's crystallographic structure, crystallinity, phase identification, and structural parameters after the weld [29].

The XRD pattern shows characteristics of the amorphous nature of ABS with the broad, diffuse peaks (Fig. 12). A typical amorphous halo is observed around 2θ = 16-20° in the base sample. A broad, peakless hump in the low-angle region (typically below 20° 2θ) indicates the amorphous content of ABS. This suggests that there is disorder in the molecular structure at lower intervals. Reduction of peaks may indicate a smaller

crystallite size or a larger structural misalignment of the polymer matrix. Narrow peaks with good definition in the high-angle region (typically above 20° 2θ) are attributed to the crystalline phase of ABS in Figs. 13 and 14. These summits are owing to ordered molecular orientation in areas that are crystalline.

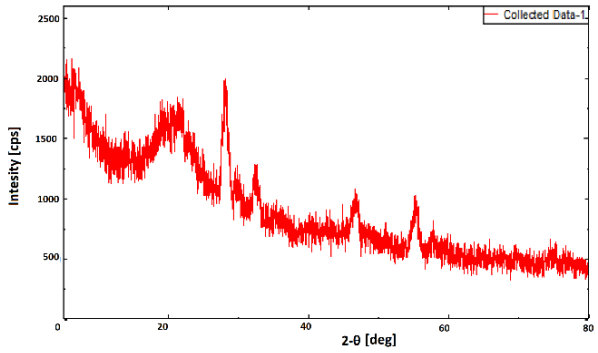

Fig. 12. XRD plot for Base Material ABS

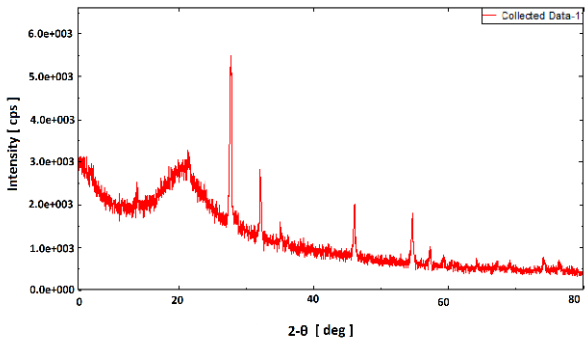

Fig. 13. XRD plot for Sample 2c

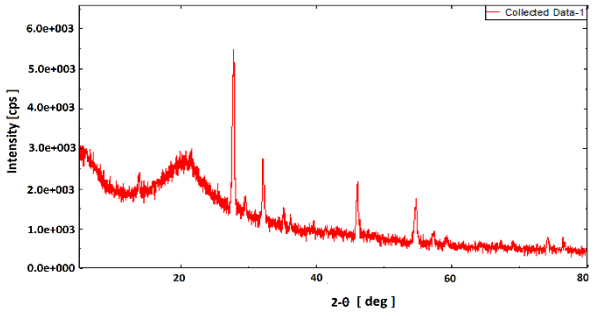

Fig.14. XRD plot for Sample 3c

The following observations were made from the XRD analysis done for two selected samples (Sample 3c and Sample 2c):

1. Exposure of the material to high-frequency vibrations causes changes in crystal orientation, grain size, and the formation of new crystalline phases.
2. Changes in peak intensity or broadening can indicate defects caused by the welding process and fluctuations in crystallite size or orientation. A decrease in crystallinity may indicate thermal degradation, chain scission, or disruption of polymer chains by welding-induced forces of thermal or mechanical stress.
3. Peaks or shifts in peak positions compared to established reference materials give information concerning the composition and nature of secondary phases present in the weld sample. There are other crystalline phases, like fillers, additives, or impurities, in addition to the ABS polymer.
4. Variations in peak intensities or broadening could be due to changes in crystallographic texture resulting from the welding process, e.g., preferential orientation along particular axes or planes. Texture analysis can provide a weld sample's mechanical properties, anisotropy, and structural integrity.

3.4 SIMULTANEOUS THERMAL ANALYSIS

For the reliability of using welded ABS materials, due to their poor thermal stability and high flammability, there is a need to evaluate the fire behaviour of ABS, specifically the ignition temperature, heat release rate, and flame spread. Simultaneous thermal analysis (STA) involves two kinds of tests run simultaneously: thermogravimetric analysis (TG) and differential scanning calorimetry (DSC) [7,27,29].

When a thermal gradient occurs in the ABS material, the onset temperature for samples 2c in Fig. 15 and 3c in Fig. 16 is 357.7˚C and 330.3˚C, respectively. The thermal decomposition is observed to happen in two steps: 250˚C and 480˚C. The DTA curve reveals at least two overlapping peaks during the initial degradation step, indicating that this first degradation process involves multiple co-occurring reactions rather than a single chemical reaction.

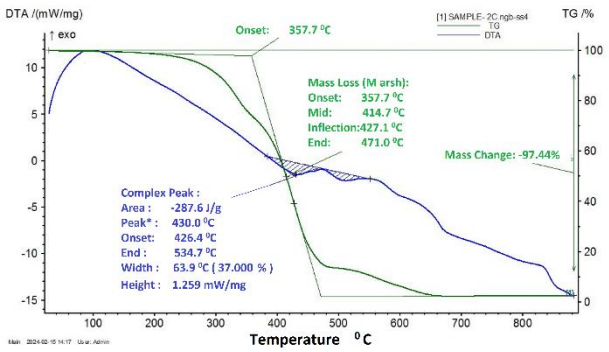

Fig. 15. TG DTA Curve for sample 2c

Fig. 16 shows slight variations in the results, that may stem from variations in process parameters such as weld time and static pressure.

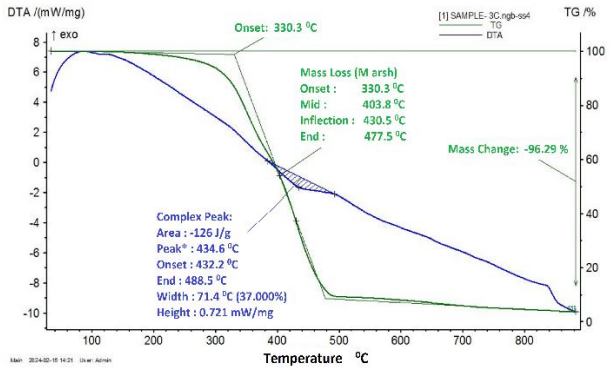

Fig. 16. TG DTA Curve for sample 3c

TG/DTA curves for ABS material battery charger casing yield the following conclusions.

1. Low-onset thermal deterioration is indicated by a decrease in onset temperature. This may be due to polymer matrix deterioration, contamination, or changes in material composition. Under thermal stress, thermal stability decreases and degradability increases.
2. Changes in TGA or DTA curve maximum positions indicate ABS polymer degradation dynamics. Different material composition, thermal history, or production conditions may cause it.

ABS polymer typically undergoes multistage decomposition, characterized by distinct weight loss steps corresponding to the degradation of different polymer constituents

3.5 ATOMIC FORCE MICROSCOPIC (AFM) ANALYSIS

AFM scans a sharp probe (or cantilever) across the material's surface. The interactions between the probe and the surface (van der Waals forces, electrostatic forces, etc.) cause the probe to deflect, and this deflection is used to generate a highly detailed topographical map of the surface at a nanometer scale. The following in Figs. 17-19, are the AFM images obtained for the samples that are characterized as Poor weld, Partial weld and Complete Weld.

Significant surface irregularities like fractures, cavities, or delamination are visible in AFM pictures in Fig. 17, of poor welds, indicating inadequate bonding at the polymer interface. Higher RMS values for weak welds indicate poor surface cohesiveness, which may be brought on by contamination, insufficient pressure, or overheating during the welding process. Areas of irregular surface topography with gaps or seams are revealed by AFM analysis of incomplete welds.

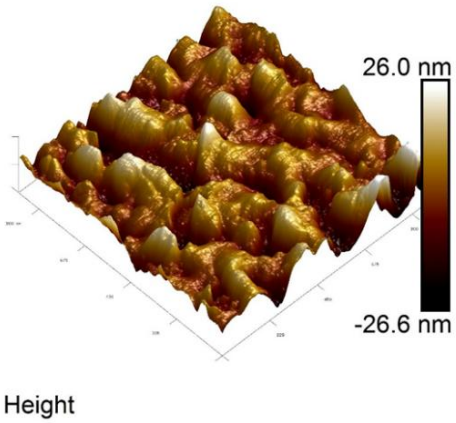

Fig. 17. AFM for poor weld

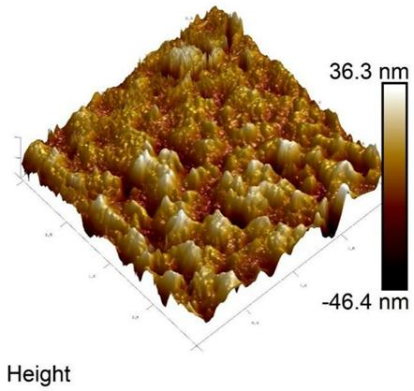

Fig. 18. AFM for partial weld

These flaws point to either inadequate heat application during welding or incomplete fusion. Higher roughness values and localized regions of heightened surface features are characteristics of partial welds in Fig. 18, which are suggestive of incomplete polymer interdiffusion.

AFM is particularly useful in determining whether the welding process has achieved sufficient intermolecular bonding. The AFM image of a complete weld sample in Fig. 19 displays a consistent surface shape with low levels of surface roughness.

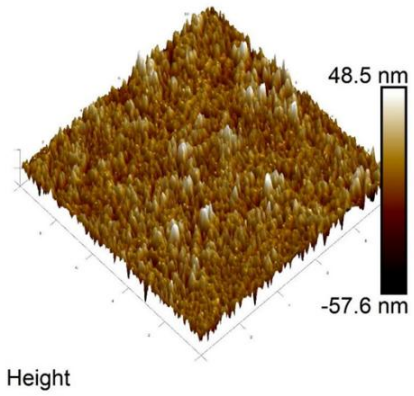

Fig. 19. AFM for full weld

4. DISCUSSION

The SEM microstructure showed the dispersed phases, indicating the rubbery particles inside the ABS. At lower magnifications, there were no visible gaps at the interface between the welded sections, indicating a successful weld with close surface contact. SEM Images indicated a reorientation of the polymer chains close to the weld, which influences the joint's structural characteristics. At the weld, some porosity was found, which could be the result of trapped air or insufficient melting.

FTIR Analysis indicates that the polymer structure remains unaltered, but localised heating affects mechanical and thermal properties. As per the XRD Analysis, shifts in peak location or broadening of peaks are indicative of the existence of residual stresses due to the welding operation, e.g., thermal expansion, contraction, or mechanical deformation.

TGA analysis noted differences in weight loss profiles, such as rates and extents of degradation, which reflect variations in the thermal stability and decomposition kinetics of different polymer components within the ABS polymer matrix. Since AFM offers nanometre-scale resolution, which is superior to other microscopy techniques. These observations are significant for the optimization of weld parameters and to ensure the required material performance in applications.

5. CONCLUSIONS

This study has thoroughly analysed the influence of welding parameters on the quality of ABS parts for the battery charger casing, joined through ultrasonic welding. The investigation has yielded significant findings using a combination of non-destructive characterization techniques.

Observations made using several characterisation techniques reveal that ultrasonic welding induces microstructural and thermal modifications in ABS. Analysis based on SEM and AFM identified localized chain reorientation and nanoscale porosity at the weld interface, which indicated incomplete polymer homogenization. Thermal cycle residual stresses were established by XRD and SEM interfacial discontinuities. FTIR indicated maintained polymer chemistry but localised property changes, whereas TGA demonstrated variable thermal degradation kinetics in ABS components, possibly aggravated by welding-induced phase separation.

Unoptimized Ultrasonic welding can impair the weld material in three ways:

- Reduced joint durability due to porosity and partial fusion.
- Thermal-mechanical welding cycles increase internal residual stresses and strains, reducing dimensional stability.
- Altered breakdown kinetics reduce thermal resilience.

These factors explain the necessity for optimised amplitude, pressure, and cooling parameters to reduce flaws and stress. To avoid porosity-induced failures in ultrasonic welded materials, welding energy must be precisely controlled. This will result in limited residual stress, which helps in ensuring dimensional accuracy. Thermal stability with controlled welding results in minimal device warping.

Further research work on ultrasonic welding (UW) should involve the use of advanced optimization techniques to minimize trial-and-error processes, which will further reduce time and energy consumption in the welding process. Real-time digital twin monitoring is one technique that can be explored to dynamically modify parameters to suit the weld characteristics. Standardization of testing and characterization methods is essential for consistent assessment of weld quality and performance.

ACKNOWLEDGEMENTS

The authors sincerely thank Mr Alwin Raj Lobo, CEO, UltraTechSonic Solutions Ltd., Bangalore, for extending the research facilities for carrying out this research.

CONFLICTS OF INTEREST

The authors declare no conflict of interest.

REFERENCES

[1] H. Li, C. Chen, R. Yi, Y. Li, J. Wu, Ultrasonic welding of fiber-reinforced thermoplastic composites: a review. *The International Journal of Advanced Manufacturing Technology,* 120, 2022: 29-57. https://doi.org/10.1007/s00170-022-08753-9

[2] E. Tsiangou, S.T. de Freitas, I.F. Villegas, R. Benedictus, Investigation on energy director-less ultrasonic welding of polyetherimide (PEI)- to epoxy-based composites. *Composites Part B: Engineering*, 173, 2019: 107014. https://doi.org/10.1016/j.compositesb.2019.107014

[3] A. Vendan Subbiah, M. Chaturvedi, K.A. Ramesh Kumar, R. Sharanabasavaraj, K. Hammoodi, A. Elsheikh, A synergistic approach to material analysis and power source engineering in ultrasonic welding of polymers. *Proceedings of the Institution of Mechanical Engineers, Part B: Journal of Engineering Manufacture*, 0(0), 2025. https://doi.org/10.1177/09544054251318078

[4] P. Yadav, Manisha, P. Gaur, Electromechanical modeling and piezoelectric vibration-based energy harvester simulation interfaced with MPPT-based electrical circuit using Matlab Simulink. *International Journal of Recent Technology and Engineering (IJRTE),* 8(2S11), 2019: 36-40. http://doi.org/10.35940/ijrte.B1007.0982S1119

[5] Z. Zhang, X. Wang, Y. Luo, Z. Zhang, L.Wang, Study on the heating process of ultrasonic welding for thermoplastics. *Journal of Thermoplastic Composite Materials,* 23(5), 2010: 647–664. https://doi.org/10.1177/0892705709356493

[6] J. Xu, R. Huanhuan, Design and finite element simulation of an ultrasonic transducer of two piezoelectric discs. *Journal of Measurements in Engineering*, 5(4), 2017: 266-272. https://doi.org/10.21595/jme.2017.19396

[7] M.A. Dundar, G.S. Dhaliwal, E. Ayorinde, M. Al-Zubi, Tensile, compression, and flexural characteristics of acrylonitrile–butadiene–styrene at low strain rates: Experimental and numerical investigation. *Polymers and Polymer Composites,* 29(5), 2020, 331-342. https://doi.org/10.1177/0967391120916619

[8] R. Bhaskar, J. Butt, H. Shirvani, Investigating the properties of ABS-based plastic composites manufactured by composite plastic manufacturing. *Journal of Manufacturing and Materials Processing*, 6(6), 2022: 163. https://doi.org/10.3390/jmmp6060163

[9] T. Chinnadurai, N. Prabaharan, S. Saravanan, M.K. Pandean, P. Pandiyan, H.H. Alhelou, Prediction of process parameters of ultrasonically welded PC/ABS material using soft-computing techniques. *IEEE Access*, 9, 2021: 33849-33859. https://doi.org/10.1109/ACCESS.2021.3061657

[10] S.A. Vendan, M. Natesh, A. Garg, L. Gao, Confluence of multidisciplinary sciences for polymer joining. *Springer*, Singapore, 2019. https://doi.org/10.1007/978-981-13-0626-6

[11] A. Alonso, M. Lázaro, D. Lázaro, D. Alvear, Thermal characterization of acrylonitrile butadiene styrene-ABS obtained with different manufacturing processes. *Journal of Thermal Analysis and Calorimetry*, 148, 2023: 10557–10572. https://doi.org/10.1007/s10973-023-12258-2

[12] E. Werner, U. Güth, B. Brockhagen, C. Döpke, A. Ehrmann, Examination of polymer blends by AFM phase images. *Technologies*, 11(2), 2023: 56. https://doi.org/10.3390/technologies11020056

[13] P. Davari, N. Ghasemi, F. Zare, Power converters design and analysis for high power piezoelectric ultrasonic transducers. *16th European Conference on Power Electronics and Applications,* 26-28 August 2014, Lappeenranta, Finland, pp.1-9. https://doi.org/10.1109/EPE.2014.6910986

[14] W.H. Kim, E.J. Kang, D.S. Park, Evaluation of welding performance of 20 kHz and 40 kHz ultrasonic metal welding. *IOP Conference Series: Materials Science and Engineering, International Conference on Structural, Mechanical and Materials Engineering (ICSMME 2017)*, Vol.248, 13–15 July 2017, Seoul, South Korea, p.012013. https://doi.org/10.1088/1757-899X/248/1/012013

[15] S. Tutunjian, M. Dannemann, F. Fischer, O. Eroğlu, N. Modler, A control method for the ultrasonic spot welding of fiber-reinforced

thermoplastic laminates through the weld-power time derivative. *Journal of Manufacturing and Materials Processing,* 3(1), 2018: 1. https://doi.org/10.3390/jmmp3010001

[16] R. Rashli, E.A. Bakar, S. Kamaruddin, Determination of ultrasonic welding optimal parameters for thermoplastic material of manufacturing products. *Jurnal Teknologi-Sciences & Engineering,* 64(1), 2013: 19–24. https://doi.org/10.11113/JT.V64.1158

[17] A. Milewski, P. Kluk, W. Kardyś, P. Kogut, Modelling and designing of ultrasonic welding systems. *Archives of Acoustics,* 40(1), 2015: 93-99.

[18] C. Volosenc, Control system for ultrasonic welding devices. *2008 IEEE International Conference on Automation, Quality and Testing, Robotics,* 22-25 May 2008, Cluj-Napoca, Romania, pp.135-140. https://doi.org/10.1109/AQTR.2008.4588809

[19] S. Rajakumar, S. Kavitha, T. Sonar, Optimization of ultrasonic welding parameters to maximize the tensile shear fracture load bearing capability of lap welded ABS plastic sheets. *International Journal on Interactive Design and Manufacturing*, 18, 2024: 3207–3216. https://doi.org/10.1007/s12008-023-01481-8

[20] L. Yang, L. Yang, Digest ultrasonic welding I: Localized heating and fuse bonding. *Engineering. arXiv*, 2023. https://doi.org/10.48550/arXiv.2301.05810

[21] I.F. Villegas, Ultrasonic welding of thermoplastic composites. *Frontiers in Materials,* 6, 2019: 291. https://doi.org/10.3389/fmats.2019.00291

[22] Y. Yang, Z. Liu, Y. Wang, Y. Li, Numerical study of contact behavior and temperature characterization in ultrasonic welding of CF/PA66. *Polymers,* 14(4), 2022: 683. https://doi.org/10.3390/polym14040683

[23] D. Rogale, S. Fajt, S. Firšt Rogale, Z. Knezić, Interdependence of technical and technological parameters in polymer ultrasonic welding. *Machines*, 10(10), 2022: 845. https://doi.org/10.3390/machines10100845

[24] C.-C. Kuo, Q.-Z. Tsai, D.-Y. Li, Y.-X. Lin, W.-X. Chen, Optimization of ultrasonic welding process parameters to enhance weld strength of 3C power cases using a design of experiments approach. *Polymers*, 14(12), 2022 : 2388. https://doi.org/10.3390/polym14122388

[25] S.A. Vendan, T. Chinnadurai, K.S. Kumar, N. Prakash, Investigations on mechanical and structural aspects of ultrasonic hybrid polymer mixture welding for industrial applications. *The International Journal of Advanced Manufacturing Technology,* 93,2017: 89–102. https://doi.org/10.1007/s00170-015-7773-z

[26] A. Benatar, M. Marcus, Chapter 11 - Ultrasonic welding of plastics and polymeric composites. In Woodhead Publishing Series in Electronic and Optical Materials, Power Ultrasonics (Second Edition). *Woodhead Publishing*, 2023: 205-225. https://doi.org/10.1016/B978-0-12-820254-8.00006-3

[27] S. Yang, J.R. Castilleja, E.V. Barrera, K. Lozano, Thermal analysis of an acrylonitrile butadiene styrene/SWNT composite. *Polymer Degradation and Stability*, 83(3), 2004: 383-388. https://doi.org/10.1016/j.polymdegradstab.2003.08.002

[28] M. Natesh, L. Yun, S.A. Vendan, K.R. Kumar, L. Gao, X. Niu, X. Peng, A. Garg, Experimental and numerical procedure for studying strength and heat generation responses of ultrasonic welding of polymer blends. *Measurement,* 132, 2019: 1-10. https://doi.org/10.1016/j.measurement.2018.09.043

[29] G. Nabi, N. Malik, M.B. Tahir, W. Raza, M. Rizwan, M. Maraj, A. Siddiqa, R. Ahmed, M. Tanveer, Synthesis of graphitic carbon nitride and industrial applications as tensile strength reinforcement agent in red acrylonitrile-butadiene-styrene (ABS). *Physica B Condens Matter*, 602,2021: 412556. https://doi.org/10.1016/j.physb.2020.412556